Macromolecules
ARTICLE

Macromolecules **2010**, *43*, 5083–5093 **5083**
DOI: 10.1021/ma100481s

Controlled Release from Polyurethane Nanocapsules via pH-, UV-Light- or Temperature-Induced Stimuli

Eva-Maria Rosenbauer, Manfred Wagner, Anna Musyanovych,* and Katharina Landfester*

Max Planck Institute for Polymer Research, Ackermannweg 10, 55021 Mainz, Germany

Received March 2, 2010; Revised Manuscript Received April 27, 2010

ABSTRACT: Polyurethane nanocapsules consisting of an aqueous core and a polymeric shell with included azo bonds as obtained via interfacial polyaddition of the monomers toluene-2,4-diisocyanate (TDI) and an azo-containing containing diol (VA-060) in inverse miniemulsion allow the selective release of encapsulated material by stimuli such as temperature, UV light, or pH change. The capsule degradation was detected by measuring time-dependently the fluorescence intensities of the dye sulforhodamine SR101, which is dissolved as the fluorescent marker in the core, by exposing the capsules to the different stimuli. Furthermore, the capsules were characterized by transmission electron microscopy (TEM) and dynamic light scattering (DLS). The main components during the capsules' degradation were determined via nuclear magnetic resonance (NMR) spectrometry exemplary directly on the azo-monomer VA-060. The results present proof-of-principle studies of different controlled releases with a prototype of polyurethane capsules using the fluorescence dye sulforhodamine SR101 as a model system.

Introduction

Polymeric capsules offer an increasing interest in the research and development for the delivery of encapsulated materials. Much effort has been focused on the design of well-defined carriers loaded with catalysts, enzymes, or drugs, which have tailored physicochemical and mechanical properties to release the material selectively at the desired target. The regulation of the release is sufficient and useful to catalyze chemical or biological reactions in certain areas. Therefore, it is necessary to activate its content or release the encapsulated material remotely. Typical release mechanisms are based on triggered systems such as pH,[1,2] laser light,[3−6] ultrasound,[7−9] temperature,[10] or enzymatic degradation.[11]

By now, a variety of the release systems have already been realized using gels,[12,13] polymeric micelles,[14−16] liposomes,[17,18] colloids,[19] and polyelectrolyte multilayer microcapsules[20] as carriers. The formation of the polyelectrolyte multilayer capsules with the desired material embedded in its core is based on the layer-by-layer (LbL) technique, depositing an oppositely charged polyelectrolyte multilayer onto the surface of a sacrificial core. The thickness of the capsule shell can be adjusted by the number of layer-by-layer deposition cycles and the size of the capsule depends on the colloidal template size. Capsules with diameters in the micrometer range up to 10 μm were obtained; in rare cases, the capsules were smaller.[21−24] This technique is already established to release the encapsulated material selectively by pH change, ultrasound, or laser light. Sukhorukov et al. have used a laser-mediated remote release of encapsulated fluorescently labeled polymers from nanoengineered polyelectrolyte multilayers containing a gold sulfide core and gold particles in their wall.[25] In further studies, the authors used laser irradiation for the release of dye-labeled dextran inside a living cell, which was encapsulated in poly(styrenesulfonate) (PSS)/poly(diallyldimethylammonium chloride) (PDADMAC) microcapsules.[3]

*Corresponding authors. (K.L.) E-mail: landfester@mpip-mainz.mpg.de. Telephone: +49(0)6131 379-130. Fax: +49(0)6131 379-330. (A.M.) E-mail: musyanovych@mpip-mainz.mpg.de. Telephone: +49(0)6131 379-248. Fax: +49(0)6131 379-100.

Dejugnat et al. investigated hollow polyelectrolyte microcapsules with the wall consisting of poly(allylamine hydrochloride) and sodium poly(styrenesulfonate). Various core templates such as manganese and calcium carbonate particles or polystyrene latexes were used.[1] These polyelectrolyte multilayers respond to a change of pH, leading to a swelling of the capsules under basic and shrinking under acidic conditions. Increasing the number of layers or the molecular weight of the polymer allows a rigidification of the structure and modification of the pH response.

Recently, a novel method, based on the "click" chemistry, has been introduced for the encapsulation of a variety of chemical and biological substances. The capsule network is also based on the LbL technique, but in addition with the Cu^{I}-catalyzed triazole formation between azides and alkynes, known as the Huisgen 1,3-dipolar cycloaddition reaction.[26−32] Caruso et al. reported about this "click" chemistry using nondegradable poly(acrylic acid) modified with azide and alkyne moieties to form polyelectrolyte multilayers.[33−35] Biocompatible multilayers are prone to enzymatic degradation and drug release from such multilayer can be considered as "triggered release".[36]

Another method to release materials from a carrier is to apply ultrasound. Goldenstedt et al. encapsulated an active agent, ethyl benzoate, in gelatin−arabic gum (acacia) based polymeric microcapsules by complex coacervation as already extensively described by Jegat and Taverde.[37] The selective delivery of the encapsulated material was obtained using a piezo-composite shock wave generator.[38]

In another strategy, Ha et al.[39] synthesized pH-sensitive poly(acrylamide-*co*-2-acrylamido-2-methyl-1-propansulfonic acid-*co*-acrylamidoglycolic) hydrogel pellets by free radical copolymerization. The hydrogels showed a sharp change in their water absorbency and molecular weight with a change in pH of the surrounding media.

The ionizable functional groups lead to a typical pH-sensitive swelling behavior, i.e. low swelling ratios at low pH and high at high pH. The pH dependence of the gels provides a biological on−off switch mechanism, which can be useful for a controlled release of the embedded material.

Published on Web 05/12/2010

Almost all methods described above are based on capsules and polyelectrolyte multilayers in the micrometer scale (range over 500 nm). There are hardly any investigations in the nanometer scale. The inspiration of the following work is the formation of capsules in the nanometer range and a defined triggered release of water-soluble encapsulated material by different stimuli. The choice of monomers/polymers and chemical reactions, which can be utilized in a miniemulsion process to form the nanocapsules with a hydrophilic or hydrophobic core, are numerous. Therefore, this technique gives the opportunity to produce capsules with desired properties for a broad range of applications. The size of the droplets mainly depends on the type of an effective amount of the surfactant used.

Recently, polyurethane nanocapsules with an aqueous core were successfully prepared performing interfacial polyaddition reaction in inverse miniemulsion system[40,41] in a controlled manner in the size range from 50 to 500 nm. The polyurethane nanocapsules could already easily be loaded with contrast agent materials such as Magnevist and Gadovist inside the core for the use in magnetic resonance imaging (MRI).[42] So, with a choice of monomers the use of these capsules as carriers for controlled release is obviously given. The miniemulsion process was also use to encapsulate azo components in a core which could be—temperature-induced—brought to a fast decomposition and led to a breakage of the nanocapsules.[43]

In this paper, stimuli-responsive polyurethane nanocapsules with an encapsulated fluorescent dye as a model system are presented. The shell is formed by interfacial polyaddition in inverse miniemulsion using toluene-2,4-diisocyanate (TDI) as hydrophobic and the azo-containing diol 2,2′-azobis{2-[1-(2-hydroxyethyl)-2-imidazolin-2-yl]propane}dihydrochloride (VA-060) as hydrophilic monomeric component. The azo component is now located in the shell and a decomposition of the azo component lead directly to a breakage of the shell. The capsule opening, and therefore the time-dependent dye release behavior of the encapsulated material by the influences of UV light, temperature, and pH-change as stimuli are studied in detail.

Experimental Section

Materials and Methods. 2,2′-Azobis{2-[1-(2-hydroxyethyl)-2-imidazolin-2-yl] propane} dihydrochloride (VA-060, Wako), 1,6-hexanediol (HDol, Fluka), toluene-2,4-diisocyanate (TDI, 98%, Aldrich), cyclohexane (HPLC-grade), and sodium chloride were used without further purification. Sodium dodecyl sulfate (SDS, 99% Merck) and LubrizolU (polyisobutylene−succinimide pentamine, M_w = 384−875 g·mol^{-1}, determined from GPC, HLB < 7, containing 50:50 wt/wt % mineral oil as a diluent, Lubrizol, France)[44] were used as surfactants. Sulforhodamine SR101 (BioChemika, for fluorescence, Fluka), was utilized as a hydrophilic fluorescent marker and as model encapsulated material. Demineralized water was used as aqueous phase throughout the experiments.

Preparation of Polyurethane Capsules. For the synthesis of the polyurethane capsules, 270 mg (0.64 mmol) of VA-060 or 76 mg (0. 64 mmol) of HDol, 0.750 g of water (pH = 6.5) or 0.750 g of sulforhodamine solution (2.0 mmol, pH 7.0) and 3.5 mg sodium chloride, which should form the hydrophilic liquid cores, were homogenized at room temperature. The different mixtures were added to 6 g of cyclohexane containing 50 mg of LubrizolU. After stirring for 1 h with a magnetic stirrer for pre-emulsification, the miniemulsion was prepared by ultrasonicating the mixture for 180 s at 70% amplitude (Branson sonifier W450 Digital, tip size 6.5 mm) under ice cooling in order to prevent polymerization. Then 170 mg (0.96 mmol) of TDI dissolved in 4 g of cyclohexane were drop-wisely added to the miniemulsion. The reaction was carried out for 24 h at 25 °C. The redispersion of the nanocapsules in the aqueous phase was performed by mixing 1.0 g of the synthesized nanocapsules/cyclohexane dispersion with 5 g aqueous solution of SDS (0.02 mol·L^{-1}) for the capsule cores prepared with sulforhodamine solution. In the case of the nanocapsules cores synthesized with water, 1 g of this dispersion was mixed with 5 g aqueous SDS solution (0.02 mol·L^{-1}) containing the same amount of sulforhodamine which should be in the capsule core of 1 g nanocapsule cyclohexane dispersion. The resulting mixtures were subjected to ultrasonication for 60 s at 17% amplitude, 10 s pulse, 5 s pause (Branson sonifier W450 Digital, tip size 6.5 mm) under ice cooling, and the cyclohexane was evaporated afterward by stirring the mixture open overnight until approximately 1.0 g of the suspension was removed. The miniemulsion was continuously refilled with water to 5.0 g (final solid content approximately 1 wt %).

Characterization of Samples. The average size and the size distribution of the final polymer capsules were determined by dynamic light scattering (DLS) using a Zeta Nanosizer (Malvern Instruments), equipped with a detector to measure the intensity of the scattered light at 173° to the incident beam.

The morphology of the capsules was studied using a transmission electron microscope (TEM) (Philips EM400) operating at an accelerating voltage of 80 kV. The 5 μL of the inverse miniemulsions were diluted in 2 mL cyclohexane, while 5 μL of the redispersed samples were diluted in 4 mL demin water. The carbon coated copper grid (400 mesh) were prepared with 3 μL of the sample and air-dried overnight.

Kinetic Examinations of the Capsule Degradation Determined with Selective Dye Release from the Capsules. The kinetic experiments with the capsules were conducted as follows.

Temperature Treatment. The redispersed samples were inserted in a thermoshaker (MKR 23, HCL BioTech) and adjusted to different constant temperatures (37, 65, or 75 °C) for defined time periods between 0 and 1500 min.

Light-Induced Treatment. The capsule dispersions were irradiated with a mercury arc lamp (TQ150 Hg-Mitteldruckstrahler, Heraeus noble light) for defined time periods between 0 and 300 min.

pH-Induced Treatment. The redispersed samples were first adjusted to pH 2.5 with hydrochloric acid (0.1 M) or with sodium hydroxide (0.1 M) to pH 9, and then put into the thermoshaker (MKR 23, HCL BioTech) at 37 °C temperature for define time periods between 0 and 20 d.

The concentration of the released sulforhodamine SR101 from the capsule core was determined with a fluorescence spectrometer (NanoDrop, ND-3300, peqlab, Biotechnologie GmbH) after defined time periods during several treatments (pH change, ΔT or *hν*). Here, 3 mL samples of the different capsule dispersions were centrifuged (14000 rpm, 30 min, 25 °C), and the capsule pellet was separated from the supernatant. Then, fluorescence of the supernatant was measured. The samples were excited with white light in the range from 460 to 650 nm. The emission was then detected at a wavelength of 605 nm. Each sample was measured five times, and an average was taken. The percentage of the released dye at certain times was calculated:

$$\%\ \text{of released dye} = \frac{I_F \times 100\%}{I_W} \quad (1)$$

where I_F is the fluorescence intensity of the sample supernatant (**HDol-D/Azo-D**) and I_W is the fluorescence intensity of the reference supernatant (**Hdol-no-D/Azo-no-D**)

Studies of the Selective Decomposition of Azo-Containing Diol VA-060 under Different Conditions (ΔT or *hν* Exposure, or pH-Change) via NMR Spectroscopy. The composition of azo-containing diol VA-060 and decomposition products were analyzed using NMR-spectroscopy. VA-060 was dissolved in 5 mL DMSO-d_6 before and after different treatments and NMR spectra were measured using a DRX-500 MHz or a DRX-700 MHz NMR spectrometer (Bruker). All spectra were integrated in relation to DMSO-H-d_5, which was constant in all experiments.

Table 1. Composition of the Synthesized Nanocapsules

	Azo-D	Azo-no-D	HDol-D	HDol-no-D
D_z, nm	320	305	265	245
solid content, %	3.1		2.0	
disperse phase	azo diol (VA-060) (270 mg)		hexandiol (HDol) (76 mg)	
	SR101-solution (750 mg, 2 mmol)	demin water (750 mg)	SR101-solution (750 mg, 2 mmol)	demin water (750 mg)
	sodium chloride (3.5 mg)			
continuous phase	cyclohexane (10 g), toluene-2,4-diisocyanate (TDI) (170 mg), LubrizolU (50 mg)			
for redispersion[a]	demin water (5.0 g)	SR101-solution (5.0 g, 0.3 mmol)	demin water (5.0 g)	SR101-solution (5.0 g, 0.3 mmol)
	sodium dodecyl sulfate (0.03 mmol)			

[a] Related to 1.0 g capsule dispersion in cyclohexane.

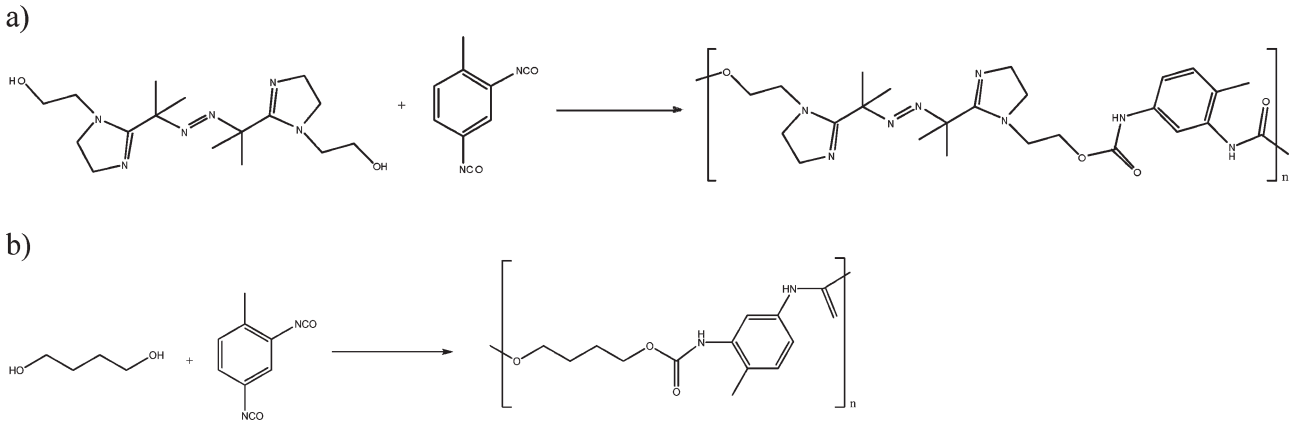

Figure 1. Main unit in the polymer after polyaddition of TDI and (a) VA-060 or (b) HDol.

Preparation of the NMR Samples for Structure Determination and Kinetic Examinations of VA-060. *Temperature Treatment*. A 10 mg sample of VA-060 was dissolved in 0.7 mL of DMSO-d_6. Kinetic investigations of the thermal decomposition products of the reaction mixture were performed using 500 MHz NMR at 60 °C in situ experiment over a time period of 18 h. During the experiment, ^{1}H NMR spectra was measured automatically every 10 min.

Light-Induced Treatment. A 10 mg sample of VA-060 was dissolved in 0.7 mL of DMSO-d_6 and exposed to a mercury arc lamp (TQ150 Hg-Mitteldruckstrahler, Heraeus noblelight). After defined time periods, ^{1}H NMR spectra were measured.

pH-Induced Treatment. A 30 mg sample of VA-060 was dissolved in 600 mg of demin water and the pH was adjusted to 2.5 with hydrochloric acid (0.1 M). Samples of 200 mg were taken after 0, 25, and 50 d. The water was removed and the solid residue of the decomposition products was dissolved in 0.7 mL of DMSO-d_6 for ^{1}H NMR measurements.

Results and Discussion

A series of nanocapsules consisting of an aqueous core and polyurethane shell were prepared by interfacial polyaddition at the water-in-oil droplets' interface as reported earlier.[40] In the beginning of the synthesis, the hexanediole (HDol) or the azo-containing diol VA-060 and sodium chloride (as osmotic pressure agent) were dissolved either in pure water or in the aqueous solution of the fluorescent dye sulforhodamine SR101. Then the mixture was added in the solution containing cyclohexane and the surfactant LubrizolU and subjected to the ultrasonication. The resulting droplets were homogeneous in size ranging between 200 and 400 nm (measured by DLS), dependent on the synthesis parameters (see Table 1). Because of the hydrophilic character of HDol and VA-060, both monomers could be dissolved inside the aqueous droplets, which were stabilized by the surfactant LubrizolU. Afterward, a solution of the hydrophobic monomer TDI in cyclohexane was drop-wisely added to the miniemulsion to start the polyaddition at the interface. Compared to water, the HDol and the VA-060 reacts faster with the isocyanate groups.[45] However, the reaction with water can not be fully avoided so that also some urea units are present in the polymer which stiffens the polymer. The polymer was formed via polyaddition reaction and precipitated simultaneously at the interfacial layer of the droplets. In addition, the surfactant LubrizolU, which contains amine end groups, can also react with the TDI and so stabilizes the capsule shell with urea units.[44] The isocyanate groups can furthermore react with water leading to the amino groups' formation, which again could then be built into the polymer by the reaction with TDI. Because of the numerous reaction possibilities of the TDI, the ratio of diol to TDI was chosen to be 1:1.5 in order to ensure enough isocyanate groups for reaction.

After the synthesis, the polyurethane capsules dispersed in cyclohexane were transferred into an aqueous solution of SDS (or SDS−sulforhodamine) in order to have a suitable environment for further, for example biomedical applications. The main urethane building unit of the polymer in the received nanocapsules synthesized either with HDol or VA-060 as monomeric diol components is shown in Figure 1.

As shown in Figure 1, the polymer obtained in the presence of VA-060 contain an azo bond incorporated in the polymeric chain. Therefore, it can be assumed that the capsule's shell, containing azo bonds, is labile and can easily break under certain conditions resulting in an opening of the capsules and release of the encapsulated components (see Figure 2).

To evaluate the total release of the encapsulated dye quantitatively, four different capsules were synthesized with water (**no-D**) or aqueous dye solution (**D**) (2 mmol of sulforhodamine) as a core

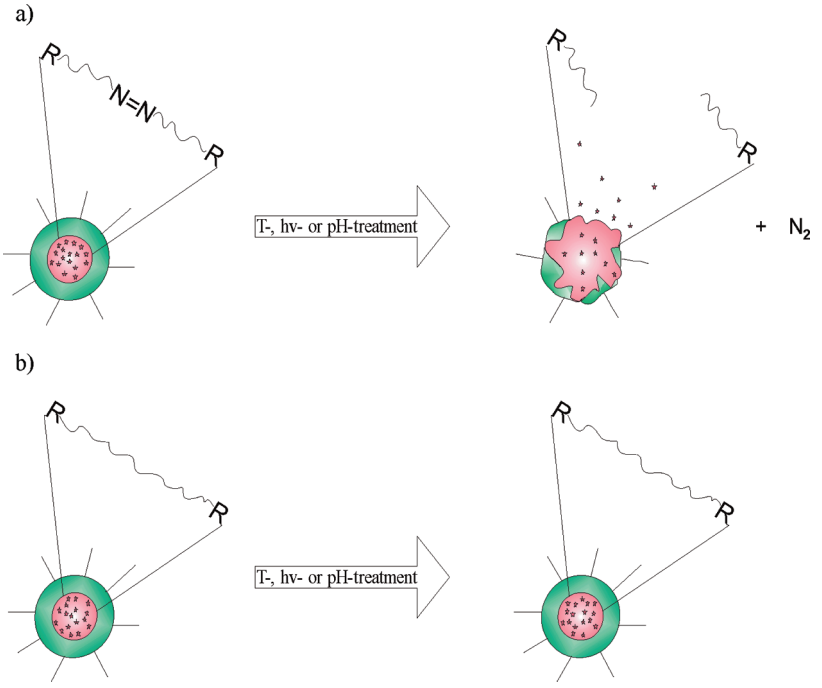

Figure 2. Schematic presentation (a) of sulforhodamine release mechanisms from nanocapsules prepared with TDI and VA-060 (**Azo-Dye**) and of (b) no sulforhodamine release from nanocapsules prepared with TDI and HDol (**Dye**).

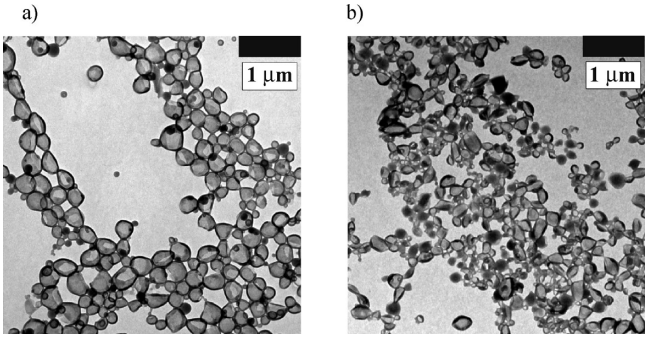

Figure 3. TEM images of polyurethane capsules obtained (a) with azo-containing diol (**Azo-D**) and (b) with diol (**HDol-D**) (both from the cyclohexane phase).

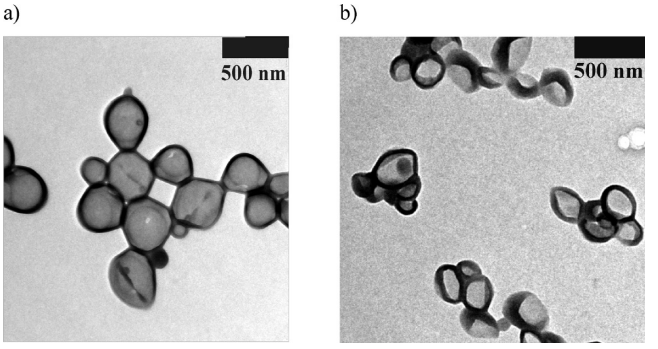

Figure 4. TEM images of polyurethane capsules obtained (a) with azo-containing diol (**Azo-D**) and (b) with diol (**HDol-D**) (both from the aqueous phase).

material using two different monomers (HDol (**HDol**) and VA-060 (**Azo**)). The capsules prepared with the dye solution (**Azo-D** and **HDol-D**) were redispersed in aqueous SDS solution, whereas the capsules synthesized with water (**Azo-no-D** and **HDiol-no-D**) as inner core were redispersed in aqueous SDS solution containing 2 mmol of sulforhodamine. The compositions of the synthesized nanocapsules are listed in Table 1.

The release of the sulforhodamine caused by the capsule's shell decomposition was calculated from the difference of the fluorescent intensities of the supernatants obtained after centrifugation of the **Azo-D** capsules and the **Azo-no-D** capsules (taken as a control for 100% release). This system was chosen in order to include the error in the calculations, which is related to the stability of the dye. An extreme light exposure or temperature treatment can lead to a photo bleaching of the dye. The fluorescence intensities during the measurements decrease significantly, but irregularly dependent on the different treatments. Therefore, this system is suited for the determination of the dye release, as the falling fluorescence intensities caused from dye treatment under different conditions, e.g., temperature, light, or pH, can be neglected.

Morphology of the Capsules. The morphologies of the obtained nanoparticles were studied by TEM. Some selected TEM images of nanocapsules in cyclohexane and redispersed in water are shown in Figure 3 and 4.

From the TEM images it can be seen that all samples exhibit a capsules structure. Stable and well-defined polymeric capsules within a size range between 200 and 400 nm are obtained with the molar ratio of 1:1.5 between HDol (or VA-060) and TDI. The polydispersity varies from 0.19 to 0.29, which indicates a relatively homogeneous size distribution for nanocapsules prepared via inverse miniemulsion. The solid contents of the **HDol-D** capsules are about 2% and for **Azo-D** capsules about 3% which in both cases corresponds well with the theoretically calculated values.

Release Kinetics from the Capsules. The prepared polyurethane capsules were exposed to different treatments in order to study their stimuli-response and release behavior. A main part of the capsule shell consists of the molecule VA-060 which is reacted via polyaddition with the cross-linker TDI (molar ratio 1:1.5). After VA-060 decomposition liberating N_2, the formed radicals recombine or disproportionate and so this reaction irreversibly destroys the capsule shell (see NMR analysis below). C, H, N analysis of the samples before and after destroying the nanocapsules by the different stimuli

show to a significant decrease of the nitrogen content in the sample by about 15% (compared to the nitrogen in the untreated sample) indicating that indeed N_2 is liberated from the system. Please note that the nitrogen from the surfactant and the urea units are still present in the sample. In the control system, no change of the nitrogen content could be detected. After a defined stimulus, the decomposition of the capsules could be also seen through a color change of the miniemulsion (Figure 5).

The morphological changes of the nanocapsules at the beginning and during the treatment under different conditions are shown in Figure 6.

After the polyaddition the capsules were spherical in shape, intact, and had a well-defined shell layer (Figure 6a). After the capsules' treatment with light or heat, the morphology is changed completely. The mercury arc lamp treatment modified the capsule structure in particle-like substructures.

For more quantitative analysis, the change in average size as a cause of capsule degradation was analyzed via DLS measurements for the capsule pairs, the **Azo-D** and control system **HDol-D**. Furthermore, the release of the encapsulated sulforhodamine dye as a function of time and treatment was evaluated using fluorescence spectroscopy.

Influence of the Temperature on the Capsule Diameter and the Sulforhodamine Release. The capsules redispersed in water were exposed to different temperatures (37, 65, and 75 °C). After different time periods the DLS measurements were performed in order to obtain preliminary information about the capsule degradation degree. The average size and size distribution, i.e. polydispersity value (PDI) of the **Azo-D** capsules were compared with those of the **HDol-D** capsules. It was found, that during the temperature treatment the capsule diameters and PDI of the different **HDol-D** capsules showed no significant change in the capsule size average distribution (±15 nm). In contrast, the PDI of the **Azo-D** capsules increases considerably particularly at higher temperatures (75 °C) (PDI > 0.65).The obtained results clearly indicate destruction and morphological changes under thermal treatment of the capsules that were synthesized with azo diol.

The amount of the released fluorescent dye from the capsules which were exposed to different temperatures (37, 65, and 75 °C), was measured after different time periods. For the analysis, the capsule's samples were centrifuged and the amount of the sulforhodamine dye in the supernatant was detected using fluorescence spectroscopy. The obtained results are shown in Figure 7.

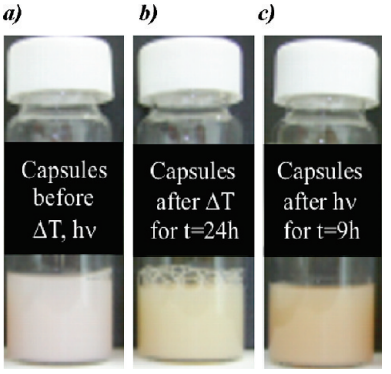

Figure 5. Color changes of the capsules dispersion after different treatments. Key: (a) without treatment, (b) thermal treatment (60 °C for 24 h), and (c) mercury arc lamp treatment for 9 h.

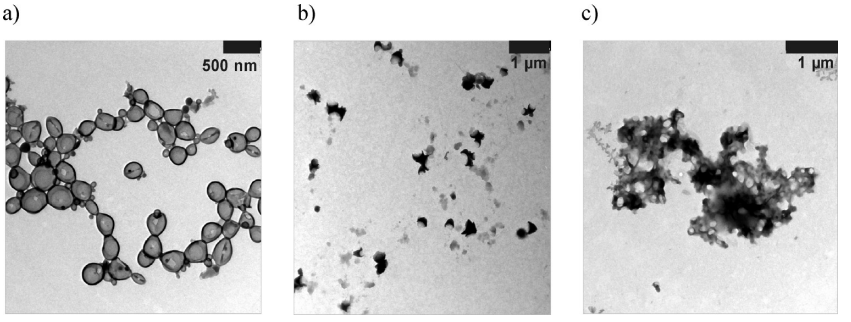

Figure 6. Morphological changes of the capsules after different treatments. Key: (a) initial capsules, (b) mercury arc lamp (9 h), and (c) temperature (60 °C, 24 h).

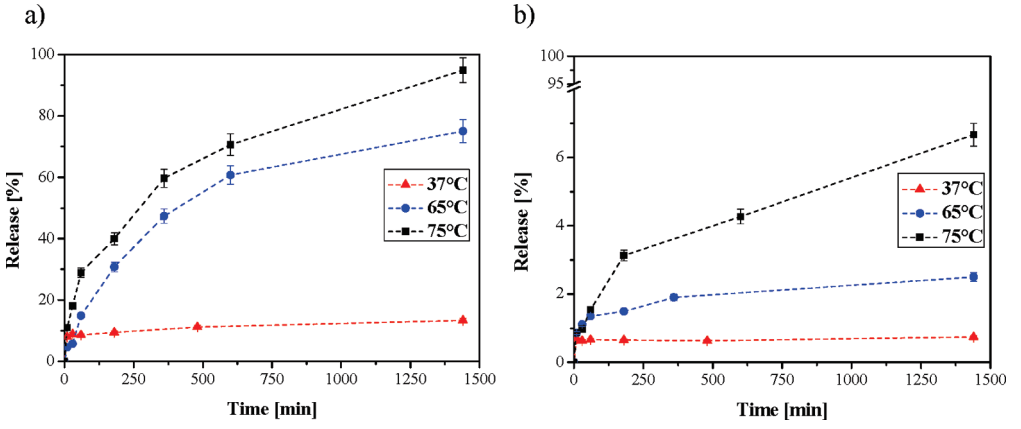

Figure 7. Release kinetics of sulforhodamine from the capsules synthesized (a) with azo-containing diol (**Azo-D**) and (b) HDiol (**HDiol-D**) as detected by the fluorescence intensity of the supernatant after centrifugation.

From Figure 7 the different sulforhodamine dye release behavior from both types of the capsules (azo- (**Azo-D**) and nonazo-containing shell (**HDol-D**) could be seen. In general, the amount of released dye increases with increasing temperature. The amount of sulforhodamine that was released from the **HDol-D** control capsules was about 1, 2, and 10 wt % after a temperature treatment at 37, 65, and 75 °C for 1500 min, respectively (see Figure 7b). In the case of azo-containing capsules (**Azo-D**) the release of the dye was about 10% at 37 °C after 24 h. However, at 65 and 75 °C more than 50% of the dye was released after 6 and 4 h, respectively. After an exposure for 25 h at 75 °C, the dye is almost completely released from the **Azo-D** capsules. The difference in the released amount of the dye molecules from azo- and nonazo containing capsules could be observed at 37 °C. This might be due to the decomposition of some azo-diol molecules during the sonication process and resulting, therefore, in a more permeable shell. The initial burst release observed mainly at 65 and 75 °C might be due to the high mobility of the dye molecules. The release behavior corresponds nicely to the change of the capsules during time. This indicates a stimuli-response mechanism of the capsule opening by decomposition which is dependent on temperature and time.

The graph of the dye release from the **Azo-D** capsules shows an exponential curve progression ($R_{(65\ °C)}^2 = 0.998$ and $R_{(75\ °C)}^2 = 0.975$) indicating a first order kinetics.

Influence of the UV Light on the Capsule Diameter and the Sulforhodamine Release. As another stimulus to open the capsules, UV light was used. The destruction of the capsules and the connected release of the dye were studied. DLS measurements were performed on the **Azo-D** and the **HDol-D** capsules at different time periods during mercury arc light exposure in order to achieve information about the homogeneity of the size changes. No significant change was found between the initial capsule diameter and the diameters after a certain time period with for all capsule samples. In case of the light exposure the **Azo-D** capsules ranging between 250 and 450 nm, while the **HDol-D** capsules varying between 175 and 320 nm during the light exposure. Therefore, the selective decomposition of the capsule shell could not be detected based on the capsule's size measurements.

The release kinetics of the dye as a function of light exposure was determined from fluorescence measurements of the supernatant after centrifugation of the nanocapsules (Figure 8).

As shown in Figure 8, a significant difference between the light induced release from the **Azo-D** and the **HDol-D** capsules is detected. It can be considered that the dye release of the **Azo-D** capsules is about ten times faster than the temperature release at 75 °C. After 5 h, more than 95% of the dye is released from the capsules. Since the capsules diameter do not change a lot, and the detected dye release was fast, it can be assumed that the nanocapsules decompose in small fraction and agglomerate to a particle-like structure. In contrast, the **HDol-D** capsules show no dye release. Even after 5 h of the light exposure the dye is still entirely encapsulated in the capsules indicating a strong, almost unbreakable polymeric shell.

Influence of the pH on the Capsule Diameter and the Sulforhodamine Release. In a next step, the release was triggered by pH change. The capsules were exposed to acidic (pH 2.5) and basic (pH 9) conditions for several days. DLS and the fluorescence intensity measurements were performed in order to obtain information about the capsule decomposition and the fluorescence dye release from the nanocapsules. The changes in PDI values of the **Azo-D** capsules were

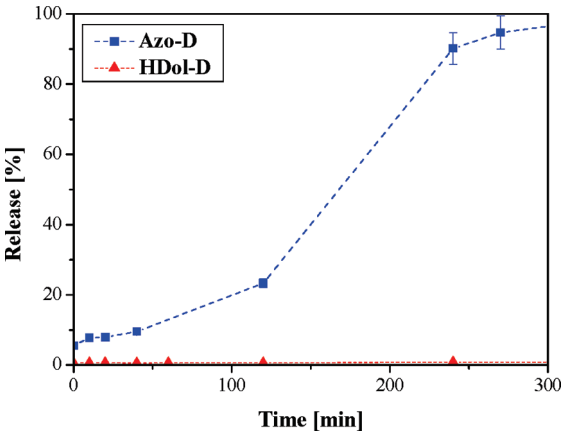

Figure 8. Release kinetics of sulforhodamine dye under light-induced exposition for the **Azo-D** and the **HDol-D** capsules as measured by the fluorescence intensity of the supernatant.

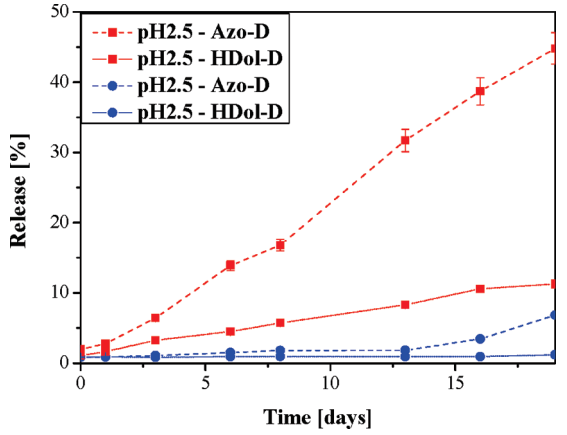

Figure 9. Release kinetics of sulforhodamine from the **Azo-D** and the control **HDol-D** capsules at different pH values (pH = 2.5 and pH = 9) as detected by the fluorescence intensity of the supernatant after centrifugation.

compared with the **HDiol-D** capsules exposing them to pH 2.5 and pH 9 over 20 d.

During 20 d, the **HDol-D** capsules do not exhibit any significant changes in the diameter and shape at any pH values. The capsules diameters vary only about 15 nm from the initial diameter (200−300 nm) and the PDI values before and after treatment were the same (0.20). Therefore, these capsules can be considered as pH resistant. The **Azo-D** capsules exposed to basic pH (pH = 9) for 20 d seem to be pH resistant as well. The size difference was found to be only around 10 nm. In contrast, the capsules exposed to acidic pH (pH = 2.5) have a massive drift and doubled in their size after 20 d. The size distribution was also broad (PDI > 0.50). The amount of the released dye from the **Azo-D** and the **HDol-D** capsules was estimated from the fluorescence measurements and the results are presented in Figure 9:

The DLS results correlate well with the results of the fluorescence measurements, indicating therefore that the shell of the **HDol-D** capsules are dense and pH resistant over a certain time period (under 10% release after 20 d). The **Azo-D** capsules are resistant at basic pH (below 15% of release after 20 d) as well, but at acidic pH the capsules release the dye constantly (linear) with almost 50% release after 20 d.

Determination of the Mechanism of the Capsules Decomposition under Different Conditions (pH, ΔT, and *hv*) via NMR on the Basis of the Azo-Containing Diol VA-060 as Model System. NMR spectroscopy was applied to study the

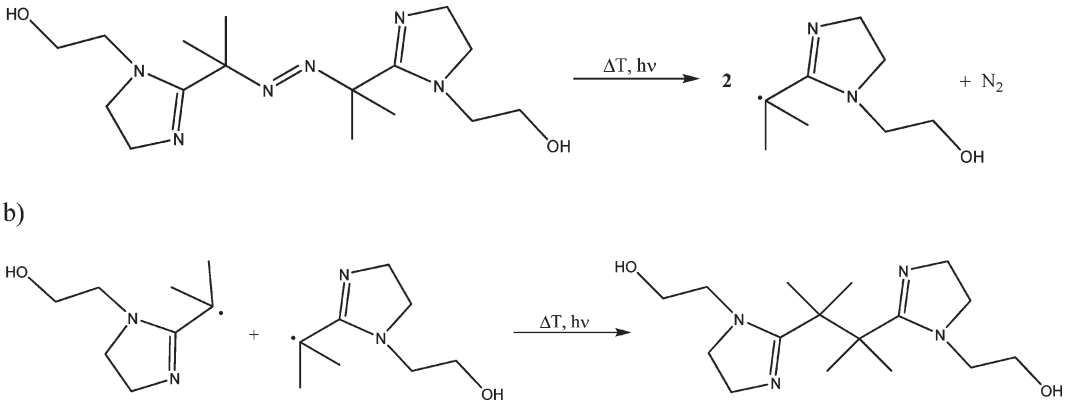

Figure 10. (a) Decomposition of VA-060 and formation of free radicals and (b) their possible recombination.

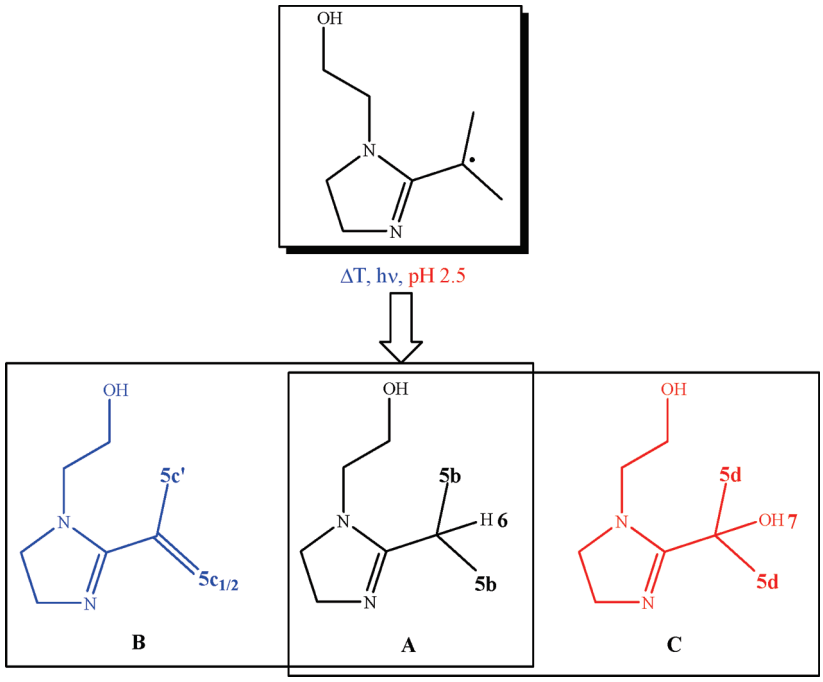

Figure 11. Main decomposition products obtained after different treatments of VA-060.

molecular mechanistic details of VA-060 destruction, which is incorporated into the shell of the polyurethane capsules. The capsules consist of the polymer made of VA-060, TDI, surfactant, and the dye. In addition, the excess of TDI leads to several side reactions with the surfactant and water. All these factors cause difficulties to analyze quantitatively the capsule opening mechanism by NMR or other methods. Therefore, the mechanism was investigated for VA-060 as model compound, which is a main part of the polymer. The molecule VA-060 has a nitrogen double bound, which is the "leaving group" under the experimental conditions and leads most probably to the destruction of the capsules. The structural changes of VA-060 after N_2 elimination under different conditions such as pH-change, temperature, or light treatment may not be equal. Therefore, it is essential to analyze each system for a better understanding and to facilitate the specific industrial/pharmaceutical applications. In addition to the structural changes of the molecule (VA-060), the monomer conversion as a function of time can also be determined quantitatively using NMR spectroscopy (see also Supporting Information).

The activation of azo-containing compounds via temperature or light induced treatments results in the release of nitrogen and formation of radicals (Figure 10a).[46] After radical formation, further steps such as disproportionation and propagation of few disproportionation products can occur, otherwise two radicals can recombine, as shown in Figure 10b.

Determination of the Main Decomposition Products of VA-060 via NMR Spectroscopic Analysis Exposing It to Different Treatments. From, the signal positions and their intensities in the NMR spectra, three main decomposition structures can be distinguished (see also Supporting Information). The analyzed products are presented in Figure 11.

The structures **A** and **B** resulting from the disproportionation of two radicals of the VA-060 decomposition product after nitrogen elimination are generated under temperature and light induced treatment. Product **C**, the structure with a heteroatom is generated together with product **A** at pH = 2.5. The illustrated structures are not only appearing in their neutral forms in the reaction mixture, but also in the protonated forms. In the following, the structures **A**, **B**, and **C** and their protonated species are discussed and characterized in detail. The remaining other substructures in the reaction mixture (over 20) are not discussed in the present paper, as they only occur in a minor percentage amount (below 5%).

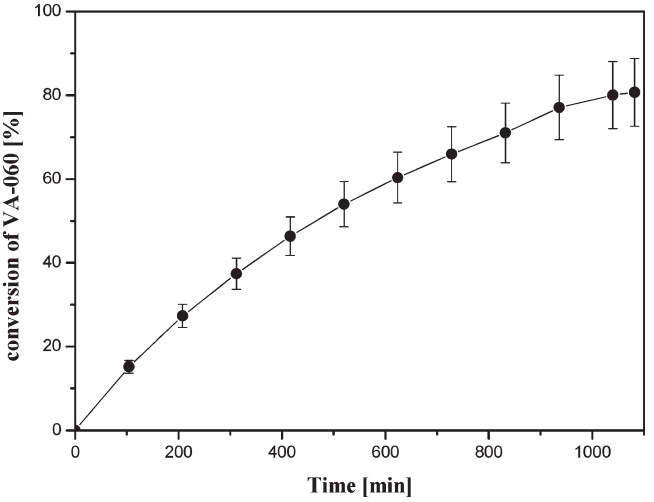

Figure 12. Decomposition of the azo-containing diol VA-060 at 60 °C as a function of time.

Determination of the Decomposition Products Prior to the Reaction. The azo-containing diol VA-060 is a reactive compound, so that storage can lead to an insignificant, but detectable decomposition. Therefore, the presence of the impurities and the amount of decomposition products before the reaction were determined in order to consider the errors in the quantitative analysis. According to the NMR spectra, it was found that about 4% of the educt VA-060 was decomposed before the reaction. Moreover, one of the main products (A) (Figure 11) is determined at a percentage of 1.3%.

Determination of the Conversion and the Ratio of the Main Products during Temperature Treatment. Kinetic investigation of the thermal decomposition products of VA-060 in DMSO-d_6 was performed using 500 MHz NMR at 60 °C over a time period of 18 h. During the experiments, ^{1}H NMR spectra were measured every 10 min.

The decomposition of the educt VA-060 was evaluated from the NMR spectra by integrating the signals of the initial protons of VA-060 (for 100% educt) and referring them to their decreasing intensities over the time under temperature treatment at 60 °C (see Figure 12).

After 18 h the decomposition of the molecule VA-060 is above 80%, whereas the decay is almost exponential ($R_{(Gauss)}^2 = 0.9975$). More than 50% of the initial VA-060 amount is already transformed in its decomposition products after 9 h. According to the half-life of VA-060 with 10 h at 60 °C,[47] the determined decomposition of VA-060 in its products is in the same range, keeping in mind that decomposition of VA-060 has already started before the reaction mixture reached 60 °C. The theoretical total decomposition of the VA-060 (about 99.99%) was determined to be after 134 h.

The main products can be quantitatively determined by integrating the corresponding proton signals in the NMR-spectra during different time periods. The main decomposition products **A** and **B** (Figure 11) are presented with a total percentage value of about 57% in the reaction mixture at every stage of the temperature treatment. The percentage ratios between both main products over the considered time are summarized in Figure 13.

According to Figure 13, molecule **A** and its protonated analogue are the mainly generated products during the temperature treatment at 60 °C. The amount increases from about 55% after 100 min up to 75% over 18 h. 60 min after the reaction has started, the amount of decomposition

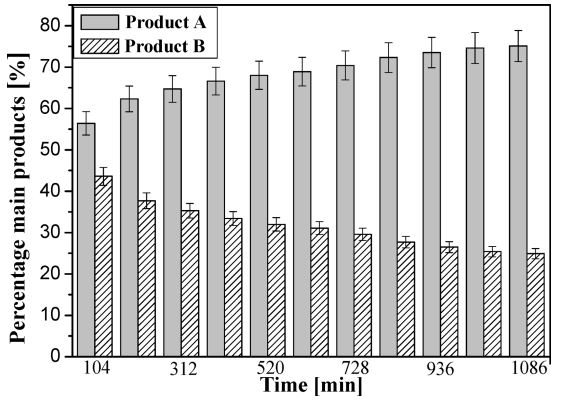

Figure 13. Percentage ratio of the main products **A** and **B** (Figure 11) for the decomposition of the azo-containing diol VA-060 at 60 °C as a function of time.

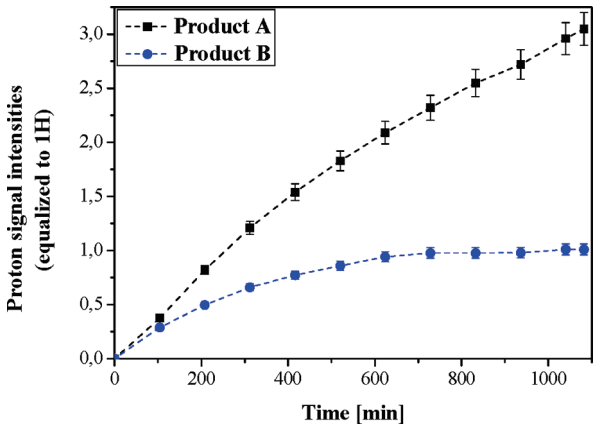

Figure 14. Proton signal intensities of the main product as a function of time obtained after VA-060 decomposition at 60 °C.

product **B** and its protonated analogue are almost equal with **A**, but slightly decreases during the next 18 h from 45% to above 30%. In Figure 14 the distribution of the proton signal intensities of the main products as a function of time is demonstrated.

As shown in Figure 14, the main decomposition product A and its protonated substructures follow almost linear increase, whereas the increase of the molecule **B** and its protonated analogue reaching a plateau after 10 h. The reason for the stagnation behavior could be some further reaction of **B**, like propagation of disproportionation products **B** with originated radical intermediate products (Figure 15) followed by termination through recombination or saturation.

The side reactions are probably in equilibrium with the generation of the decomposition products. This fact might be explained with the almost linear growth of the percentages of **A** and the slight decrease of the percentages growth of **B**.

Determination of the Conversion and the Ratio of the Main Products to Each Other during a Defined Light Exposure. In the next set of experiments, VA-060 was dissolved in DMSO-d_6 and exposed to UV light. Samples were taken after certain time periods and ^{1}H NMR spectra were measured using 500 MHz NMR.

The time−conversion of VA-060 was evaluated from the NMR spectra as described in 3.3.3. It was found that the conversion reaches about 100% already after 3.5 h. This indicates that the light induced release is more powerful than the effect of temperature. The main products from both releases are mostly alike, but their generation with the

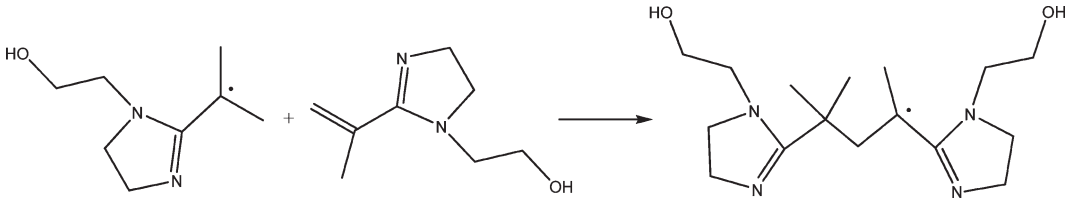

Figure 15. Growth mechanism of disproportionation products.

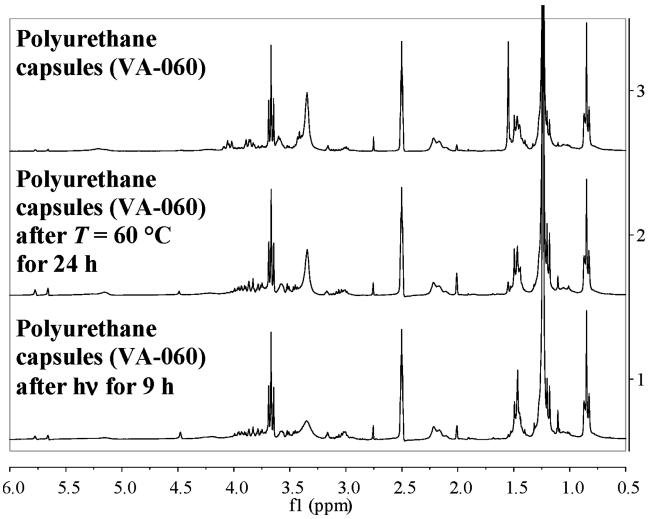

Figure 16. ^{1}H NMR (300 MHz, DMSO-d_6, 298.3 K) spectra of the azo-containing polymer nanocapsules (**Azo-D**) after different treatments.

mercury arc lamp is about 40 times faster than treating the azo containing diol at 60 °C.

The main products can be differentiated quantitatively by integrating the proton signals in the spectra at different time periods. The main products **A** and **B** (Figure 11) were generated after 3.5 h as well as after 9 h under light exposure with a percentage amount of approximately 63%. However, the ratio of the percentages compared to each other changes with light-induced treatment.

The percentage ratio distribution of main product **A** and its protonated analogues increases from 60% after 3.5 h to more than 70% after 9 h. At the same time the percentage amount of the molecule **C** decreases from 40% to 25%. The reason for these changes could be due to some rearrangement; most probably there is a transformation from the kinetically stabilized to the thermodynamically stabilized product as well as some further competitive reactions of this molecule with radicals might occur, e.g., propagation (Figure 15), followed by termination.

Determination of VA-060 Decomposition Conversion and the Ratio of the Main Products Produced during Treatment at pH = 2.5. For the examination of the azo-containing diol decomposition at acidic pH, VA-060 was dissolved in water and the pH was adjusted to 2.5 with 0.1 M hydrochloric acid. Samples were taken after 0, 25, and 50 d and separated from the water phase using centrifugation. The solid residues were dissolved in DMSO-d_6 for recording NMR spectra.

The analysis of the spectra revealed an almost 100% conversion of VA-060 in its different decomposition products already after 25 d. The average of the main decomposition products **A** and **C** (Figure 11) in the reaction mixture was about 28% after 25 d as well as after 50 d. The ratio between main products **A** and **C** does not change during this time period. Product **A** was generated with a percentage average of 76% after 25 d and after 50 d. The decomposition product **C** was found in the average of 24%. Because of the fact, that the starting materials was entirely converted after 25 d, it could be assumed, that the thermodynamically stable product has been already generated after this time period. It is interesting to note that the main difference between the temperature and light induced release to the pH-induced is that no side product **B** has been detected.

Comparison between the VA-060 Decomposition and the Capsule Degradation. The NMR spectra of the initial polymer and different decomposition products of the polymer that were generated via light, temperature, or pH treatment are shown in Figure 16.

The polymer spectra are highly complicated; even the nonredispersed initial spectrum is difficult to analyze due to the complex polymeric network structure. In addition, the surfactant LubrizolU is embedded covalently in the shell and the corresponding signals overlap with the important parts in the spectrum. Therefore, the average of the main decomposition products cannot be clearly evaluated. However, comparing the spectra of VA-060 and the polymeric network of the capsule shell before and after the light induced treatment (Figure 17), the main decomposition products as detected in the spectra can be clearly assigned.

In the spectra (Figure 17a) the signals of 12 protons at δ = 1.59 ppm (signed yellow) next to the nitrogen double bond are presented in the educt spectrum as well as in the initial polyurethane one. The initial polyurethane spectrum, Figure 17a, shows signals of the decomposition products (signed blue) as well, formed most probably by the ultrasonification treatment during the preparation of the capsules. After the light treatment the main decomposition products can be determined in the reaction mixture of VA-060 and in the polyurethane mixture, see Figure 17b. The initial signals of the 12 protons at δ = 1.59 ppm almost disappeared, so that the assurance of the nitrogen release and the decay of the polymer is given.

As seen in the TEM picture above (Figure 6), despite the low decomposition of the monomer during the preparation, the generated capsules are almost intact. After the destruction of the nanocapsules, only fragments of the shell are seen. Together with the NMR data, one can speculate that the radicals could possibly react with the analogue of the decomposition product **B** (Figure 11) to generate oligomers followed by recombination.

The temperature induced treatment at 60 °C is slower than the light induced; the total decomposition is not completed until 134 h, and an equilibrium exists between the main decomposition products. Therefore, it can be assumed that the radicals have less ability to react with a decomposition product like **B**, but a further attraction to recombine. That means a frazzle-like structure was built up from the capsules, what declared the massive increase of the hydrodynamic capsule diameter (see Figure 6c).

Finally the results of the dye release from the capsules can be compared with the results from the NMR spectra analysis of the monomer decomposition. The small variations between capsules and the monomer VA-060 degradation,

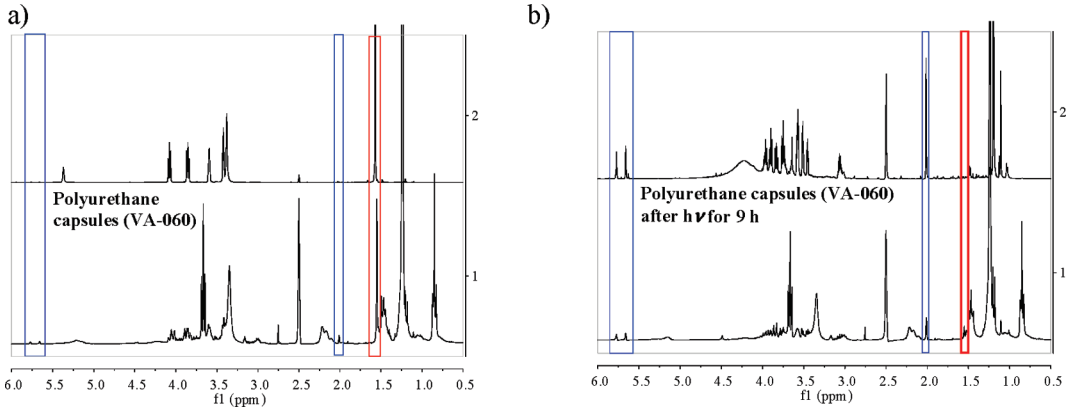

Figure 17. Comparison between VA-060 and the polyurethane capsules (**Azo-D**): (a) initial monomer and polymer; (b) decomposition products of monomer and polymer after thermal treatment.

especially at the pH induced treatment can be assigned to the reversible binding of the dye in the capsule shell. Therefore, the release is decelerated, which leads to more realistic statements for former applications where encapsulated material can interact with the capsule shell.

Conclusion

Polyurethane nanocapsules in the size range between 300 and 400 nm were prepared via polyaddition reaction in inverse miniemulsion using the hydrophilic azo containing diol 2,2′-azobis{2-[1-(2-hydroxyethyl)-2-imidazolin-2-yl]propane}dihydrochloride (VA-060) and the hydrophobic monomer toluene 2,4- diisocyanate (TDI). After the synthesis capsules were transferred into the aqueous phase. The polymeric layer decomposition can be triggered through a selective stimulus (e.g., ΔT, $h\nu$, or pH change). The capsules degradation products were investigated with the enhancement of the average diameter, morphological changes, and with the release of the sulforhodamine SR101 dye. Dependent on the type of stimulus the release of the fluorescent dye occurs in minutes (mercury arc lamp), in hours (temperature treatment), or in days (pH-induced treatment). The analysis of the molecular mechanistic details was examined using NMR spectroscopy on the model of VA-060, which is a main component of the capsule's polymeric shell. The main decomposition products and their percentage ratio were established. The results from the analysis of the capsule decomposition are comparable with the results from the NMR-spectroscopic analysis of the model VA-060.

The proof of principle for different controlled releases with a prototype of polyurethane nanocapsules was successfully presented, allowing the encapsulation and induced release of the hydrophilic materials out of the capsules. This new generation of triggered nanocapsules, therefore, opens a broad area for various potential applications where a selective release is requested. Beside the triggered release of hydrophilic drugs for biomedical needs a new route could be the usage of nanocapsules as carriers for chemical substances which could catalyze the chemical reaction. The formation of free radicals could be used in the initiation of further reactions, leading to a formation of hybrid materials, for example.

Supporting Information Available: Text giving general information about the procedures and characterizations, figures showing the structure of VA-060, NMR spectra, main decompostion products, COSY spectra, structures of the protonated subproducts, and tables of the assignments of atoms in the NMR spectra. This material is available free of charge via the Internet at http://pubs.acs.org.

References and Notes

(1) Dejugnat, C.; Sukhorukov, G. B. *Langmuir* **2004**, *20*, 7265–7269.
(2) Mauser, T.; Dejugnat, C.; Sukhorukov, G. B. *Macromol. Rapid Commun.* **2004**, *25* (20), 1781–1785.
(3) Skirtach, A. G.; Javier, A. M.; Kreft, O.; Kohler, K.; Alberola, A. P.; Mohwald, H.; Parak, W. J.; Sukhorukov, G. B. *Angew. Chem., Int. Ed.* **2006**, *45*, 4612–4617.
(4) Skirtach, A. G.; Antipov, A. A.; Shchukin, D. G.; Sukhorukov, G. B. *Langmuir* **2004**, *20* (17), 6988–6992.
(5) Radt, B.; Smith, T. A.; Caruso, F. *Adv. Mater.* **2004**, *16*, 2179–2184.
(6) Angelatos, A. S.; Radt, B.; Caruso, F. *J. Phys. Chem. B* **005**, *109*, 3071–3076.
(7) Skirtach, A. G.; De Geest, B. G.; Mamedov, A.; Antipov, A. A.; Kotove, N. A.; Sukhorukov, G. B. *J. Mater. Chem.* **2007**, *17*, 1050–1054.
(8) Postema, M.; Bouakaz, A.; de Jong, N. *Trans. Ultrasonics Ferroelectr. Freq. Control* **2005**, *52*, 1035–1041.
(9) Lentacker, I.; De Geest, B. G.; Vandenbroucke, R. E.; Peeters, L.; Demeester, J.; De Smedt, S. C.; Sanders, N. N. *Langmuir* **2006**, *22*, 7273–7278.
(10) Wang, A.; Tao, C.; Cui, Y.; Duan, L.; Yang, Y.; Li, J. *J. Colloid Interface Sci.* **2009**, *332*, 271–279.
(11) De Geest, B. G.; Vandenbroucke, R. E.; Guenther, A. M.; Sukhorukov, G. B.; Hennink, W. E.; Sanders, N. N.; Demeester, J.; De Smedt, S. C. *Adv. Mater.* **2006**, *18*, 1005–1009.
(12) Nowak, A. P.; Breedveld, V.; Pakstis, L.; Ozbas, B.; Pine, D. J.; Pochan, D.; Deming, T. J. *Nature* **2002**, *417* (6887), 424–428 .
(13) Das, M.; Mardyani, S.; Chan, W. C. W.; Kumacheva, E. *Adv. Mater.* **2006**, *18* (1), 80–83.
(14) Kwon, G. S.; Okano, T. *Adv. Drug Delivery Rev.* **1996**, *21* (2), 107–116.
(15) Allen, C.; Eisenberg, A.; Mrsic, J.; Maysinger, D. *Drug Delivery* **2000**, *7* (3), 139–145.
(16) Duncan, R. *Nat. Rev. Drug Discovery* **2003**, *2*, 347–360.
(17) Chaize, B.; Colletier, J. P.; Winterhalter, M.; Fournier, D. *Artif. Cells, Blood Subst., Immobilization Biotechnol.* **2004**, *32* (1), 67–75.
(18) Michel, M.; Winterhalter, M.; Darbois, L.; Hemmerle, J.; Voegel, J. C.; Schaaf, P.; Ball, V. *Langmuir* **2004**, *20*, 6127–6133.
(19) Faraasen, S.; Voros, J.; Csucs, G.; Textor, M.; Merkle, H. P.; Walter, E. *Pharm. Res.* **2003**, *20* (2), 237–246.
(20) Peyratout, C. S.; Dahne, L. *Angew. Chem., Int. Ed.* **2004**, *43*, 3762–3783.
(21) Caruso, F. *Adv. Mater.* **2001**, *13*, 11–22.
(22) Caruso, F.; Spasova, M.; Saigueirino-Maceira, V.; Liz-Marzan, L. M. *Adv. Mater.* **2001**, *13*, 1090–1094.
(23) Park, M. K.; Xia, C. J.; Advincula, R.; Caruso, F. *Abstracts of Papers of the American Chemical Society*; American Chemical Society: Washington DC, 2001, *Vol. 221*, 95-PMSE.
(24) Park, M. K.; Xia, C. J.; Advincula, R. C.; Schutz, P.; Caruso, F. *Langmuir* **2001**, *17*, 7670–7674.
(25) Skirtach, A. G.; Dejugnat, C.; Braun, D.; Susha, A. S.; Rogach, A. L.; Parak, W. J.; Mohwald, H.; Sukhorukov, G. B. *Nano Lett.* **2005**, *5*, 1371–1377.
(26) Lutz, J. F. *Angew. Chem., Int. Ed.* **2007**, *46*, 1018–1025.
(27) Binder, W. H.; Sachsenhofer, R. *Macromol. Rapid Commun.* **2007**, *28*, 15–54.

(28) Fournier, D.; Hoogenboom, R.; Schubert, U. S. *Chem. Soc. Rev.* **2007**, *36*, 1369–1380.
(29) Hawker, C. J.; Wooley, K. L. *Science* **2005**, *309* (5738), 1200–1205.
(30) Kolb, H. C.; Finn, M. G.; Sharpless, K. B. *Angew. Chem., Int. Ed.* **2001**, *40*, 1200–1204.
(31) Liebert, T.; Hansch, C.; Heinze, T. *Macromol. Rapid Commun.* **2006**, *27*, 208–213.
(32) Lutz, J. F.; Borner, H. G.; Weichenhan, K. *Macromol. Rapid Commun.* **2005**, *26*, 514–518.
(33) Zelikin, A. N.; Quinn, J. F.; Caruso, F. *Biomacromolecules* **2006**, *7*, 27–30.
(34) Such, G. K.; Quinn, J. F.; Quinn, A.; Tjipto, E.; Caruso, F. *J. Am. Chem. Soc.* **2006**, *128*, 9318–9319.
(35) Such, G. K.; Tjipto, E.; Postma, A.; Johnston, A. P. R.; Caruso, F. *Nano Lett.* **2007**, *7*, 1706–1710.
(36) De Geest, B. G.; Van Camp, W.; Du Prez, F. E.; De Smedt, S. C.; Demeester, J.; Hennink, W. E. *Macromol. Rapid Commun.* **2008**, *29*, 1111–1118.
(37) Jegat, C.; Taverdet, J. L. *Polym. Bull.* **2000**, *44*, 345–351.
(38) Goldenstedt, C.; Birer, A.; Cathignol, D.; Chesnais, S.; Bahri, Z. E.; Massard, C.; Taverdet, J. L.; Lafon, C. *Ultrasonics Sonochem.* **2008**, *15*, 808–814.
(39) Rao, K.; Ha, C. S. *Polym. Bull.* **2009**, *62*, 167–181.
(40) Crespy, D.; Stark, M.; Hoffmann-Richter, C.; Ziener, U.; Landfester, K. *Macromolecules* **2007**, *40*, 3122–3135.
(41) Landfester, K.; Tiarks, F.; Hentze, H. P.; Antonietti, M. *Macromol. Chem. Phys.* **2000**, *201*, 1–5.
(42) Jagielski, N.; Sharma, S.; Hombach, V.; Mailander, V.; Rasche, V.; Landfester, K. *Macromol. Chem. Phys.* **2007**, *208*, 2229–2241.
(43) Volz, M.; Walther, P.; Ziener, U.; Landfester, K. *Macromol. Mater. Eng.* **2007**, *292*, 1237–1244.
(44) Rosenbauer, E. M.; Landfester, K.; Musyanovych, A. *Langmuir* **2009**, *25*, 12084–12091.
(45) Torini, L.; Argillier, J. F.; Zydowicz, N. *Macromolecules* **2005**, *38*, 3225–3236.
(46) Linker, T.; Schmittel, M., *Radikale und Radikalionen in der Organischen Synthese*. Wiley-VCH: Weinheim, Germany, 1998.
(47) http://www.wako-chem.co.jp/specialty/waterazo/index.htm